UDC 620 . 186 . 5 : 539 . 4 . 072

Technical Report

Two-dimensional Grain Growth Simulation by Local Curvature Multi-vertex Model

Teruyuki TAMAKI* Kenichi MURAKAMI
Kohsaku USHIODA

Abstract

A local curvature multi-vertex model was developed. This model is the straightforward two-dimensional topological network model based on the physical principles which consider the curvatures of grain boundaries and the grain boundary tensions at triple junctions. The simulator based on the physical model was developed and applied to the materials with an artificial random texture and an actual texture. As the results, the grain growth by simulation obeyed the 1/2 low of time which was derived from the classical curvature model. Moreover, the grain growth velocity and misorientation distribution was turned out to be changed by the grain boundary characteristics. The developed model was verified to simulate the experimental results quite well.

1. Introduction

The properties of steel and other metallic materials depend much on their texture. Therefore, in order to impart high qualities to steel materials, it is extremely important to predict and control their texture in the manufacturing process. So far, materials and processes for prediction and control of textures have been developed based on metallurgical knowledge. With the aim of innovating the conventional method of developing materials and processes, we recently tried a new approach based on a materials physics model that would permit seeking ideal materials and processes.

In simulations in the field of materials physics called computational materials science, for example, the molecular dynamics methods and Monte Carlo methods have been used to study the dynamics of lattices and defects on an atomic scale. In materials simulations in the field of mechanical engineering, large-scale structural problems, etc. have been studied by employing the finite element method that incorporates microstructures. In contrast to those examples, in the sphere of classical materials science, that is, the meso-scale region, including textures, larger than the atomic scale and smaller than the macro scale, simulation techniques have just begun to be developed in recent years. Because meso-scale simulations handle huge space and time, they require a concept, or a physical model, which describes various physical phenomena precisely. On the other hand, thanks to remarkable enhancements in computer throughput in recent years, it has become possible to perform meso-scale simulations even without adopting a concept, which makes the model that describes the physical phenomena so abstract as to impair its physical image.

Therefore, we first created a new physical model that describes the grain growth while paying attention to the texture of metallic materials and then fabricated a simulator based on that physical model. We also discussed the validity and applicability of our model and simulator by examining the time evolution of artificial textures and comparing the experimental results with the simulation results.

2. Grain Growth Models

2.1 Conventional models

In order to describe the grain growth, various models have been proposed. The statistical model—one of those models—is used, for example, to understand the mechanisms of selective grain growth in grain-oriented silicon steel sheet in the steelmaking process.[1] This

* Chief Researcher, Hirohata R&D Lab.
1 Fuji-cho, Hirohata-ku, Himeji, Hyogo 671-1188

model is useful in that it has made possible the identification, among a huge number of matrix grains, of a limited number of very small grains, which grow into very large grains. On the other hand, it cannot be used to study, on individual grains, the texture morphology that influences the grain boundary property and pinning, which is considered to govern discontinuous grain growth. Thanks to the dramatic progress of electron backscatter diffraction (EBSD) technology in recent years,[2] it has become possible to directly observe textures so easily that fine grains that grow into huge grains can be identified relatively easily. Under that condition, developing a new technique that permits fully utilizing EBSD observation data has been called for.

As techniques to describe the grain growth, stochastic method (Monte Carlo method),[3] phase-field method,[4] topological network model (front tracking model)[5, 6] and vertex model,[7-10] have already been proposed and developed. Those methods or models are all sophisticated in that they deal with the texture morphology, and under certain limited conditions, they have successfully described the grain growth.

The stochastic method handles the grain boundary property and pinning mathematically. Therefore, it cannot sufficiently express the physical image of discontinuous grain growth.

The phase-field method, which is also applied to grain growth models, requires by nature expressing the grain boundaries by finite widths and hence, the grain boundaries blur. Therefore, in the early stages of grain growth in which there are many fine grains, the method does not always offer sufficient simulation accuracy. Besides, introducing new physical principles to triple junctions, etc., is not easy.

The topological network model approximates the grain boundaries by curved lines. Unlike the blurred grain boundaries produced by the phase-field method, this model offers clearly defined grain boundaries. On the curve between two triple junctions, several virtual vertices (double junctions) are laid out to permit calculating the local curvatures of grain boundaries. Local grain boundaries, or virtual vertices on the grain boundary, move with velocity vector $\vec{v}_{gb,\,i}$.

$$\vec{v}_{gb,\,i} = m_{gb,\,i}\,\gamma_i\,\vec{\kappa}_i \qquad (1)$$

Where $m_{gb,\,i}$ denotes grain boundary mobility; γ_i, grain boundary energy per unit length for two-dimensional systems; and $\vec{\kappa}_i$, local grain boundary curvature at virtual vertex i. On the other hand, the grain boundaries near triple junctions, or the positions of virtual vertices, are mathematically adjusted so that the grain boundaries intersect with one another at an angle at which the grain boundary tensions produced by the grain boundary energies achieve equilibrium.[5] For example, when the three boundary energies are the same, the angle of intersection is adjusted to 120 degrees.

In the initial vertex models, the grain boundaries are always approximated by straight lines.[7, 8] In those models, the driving force for grain growth is the grain boundary tension acting upon triple junctions, which move with velocity vector $\vec{v}_{triple,\,i}$.

$$\vec{v}_{triple,\,i} = m_{triple,\,i} \cdot \sum_{j=1}^{3} \gamma_{ij} \frac{\vec{r}_{ij}}{\|\vec{r}_{ij}\|} \qquad (2)$$

Where $m_{triple,\,i}$ denotes mobility of the triple junction i; γ_{ij}, grain boundary energy per unit length of grain boundary between triple junction i and triple junction j; and $\vec{r}_{ij}$, vector from triple junction i to triple junction j.[7] Energy per unit length is expressed in the same unit as tension. Therefore, $\gamma_{ij} \cdot \vec{r}_{ij} / \|\vec{r}_{ij}\|$ in Equation (2) indicates the tension acting on the triple junction. Thus, the movement of triple junctions is described accurately. However, the problem is that the grain boundaries that are ordinarily curved lines are expressed as straight lines.

The initial vertex models described above have been improved by providing virtual vertices on the grain boundaries.[9, 10] By this improvement, the grain boundaries are approximated by polygonal lines. The motion of each virtual vertex is described by a variational principle based on the Newtonian equation containing a viscosity term or a friction term. Because the improved vertex model is based on a physical principle, it is considered suitable to describe the grain growth. However, when the number of virtual vertices on the grain boundary is small, a significant error can occur because the grain boundaries are approximated not by curved lines, but by polygonal lines. For example, in the shrinkage of an isolated n-sided polygon, the moving speed of virtual vertices described by an improved vertex model is about $1/\cos(\pi/n)^2$ times faster than the moving speed calculated from the curvature obtained by a topological network model.[9] Although they become equal at the limit of $n \to \infty$, the error is as much as about 11% when $n = 10$.

Therefore, we propose a two-dimensional topological network model that permits eliminating the above problems and that expresses the physical principles in a straightforward manner.

2.2 Proposed model: local curvature multi-vertex model

2.2.1 Principle of grain boundary migration

In order to come up with a two-dimensional grain growth model that is more accurate and more straightforward than conventional models, we introduce two types of vertices using the same method as that adopted by Frost and Fuchizaki.[5, 9] One is the triple junction, which is an actual vertex. The other is a vertex on the grain boundary. It is a virtual vertex for discretization of the grain boundary. Using this method, the migration of grain boundaries expressed by a line is converted to the migration of vertices. Each virtual vertex is connected to the two adjoining vertices. On the other hand, each real vetex is connected to the three adjoining vertices. The migration of virtual vertices and real vetices follows Equations (1) and (2). The local curvature vector, $\vec{\kappa}_i$, is calculated by the following equation.

$$\|\vec{\kappa}_i\| = 1 / R_i \qquad (3)$$

Where R_i denotes the radius of a circle determined by three points, that is, vertex i and the two vertices that adjoin it. The direction of local curvature vector $\vec{\kappa}_i$ is from vertex i toward the center of the circular arc as shown in **Fig. 1**. This model can be called a local curvature multi-vertex model. Ordinarily, two adjoining circular arcs do not coincide with each other. When drawing the structure of a texture, two vertices are connected by a straight line for convenience. However, the method of local curvature calculation is different from the drawn line.

2.2.2 Validation of model

In order to confirm the validity of our proposed model, we studied the shrinkage of an isolated and closed circular grain boundary. Using a classical curvature model, it is possible to describe the shrinkage of the circle as $dr/dt = m_{bg}\ \gamma/r$, where r denotes the radius of the circle; m_{bg}, the grain boundary mobility; and γ, the grain boundary energy per unit length. The shrinking speed of the circle in the proposed local curvature model is exactly the same as the shrinking speed in the above classical curvature model. It should be noted, however, that there must be three or more virtual vertices on the circular arc in the proposed model.

2.2.3 Topological transformation

In the time evolution of grain growth, topological transformation is required. Weygand et al. have already proposed a topological transformation for their vertex model. We use that topological transfor-

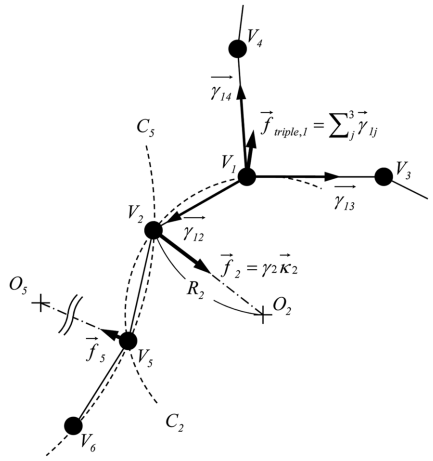

Fig. 1 Local curvature multi-vertex model
$\vec{f}_i$ and $\vec{f}_{triple,j}$ are the driving forces of virtual vertex *i* and triple junction *j* respectively in this model. V_i is the vertex *i*. C_i is circle arc determined by the vertex V_i and nearest neighbors in both sides. O_i is the center of circle arc C_i. R_i is the radius of circle arc C_i. $\vec{\gamma}_{ij}$ is the grain boundary energy vector defined by $\vec{\gamma}_{ij} = \boldsymbol{\gamma}_{ij} \cdot \vec{r}_{ij} / \| \vec{r}_{ij} \|$. $\boldsymbol{\gamma}_{ij}$ is the energy per unit length of the grain boundary between the vertices *i* and *j*. $\vec{r}_{ij}$ is the vector connecting vertex *i* with vertex *j*.

mation in our proposed model as well.[10)]

2.2.4 Grain boundary energy and grain boundary mobility

The grain boundary energy and grain boundary mobility depend on grain misorientation. Grain boundary energy γ and grain boundary mobility m around the misorientation of a coincidence site lattice (CSL) boundary are expressed by the following equations when the minimum value is 0.[11)]

$$\gamma = \gamma_m \frac{|\theta - \theta_0|}{\theta_m} \left(1 - \ln \frac{|\theta - \theta_0|}{\theta_m}\right) \quad (4)$$

$$m = m_m \left[1 - e^{-B\left(\frac{|\theta - \theta_0|}{\theta_m}\right)^n}\right] \quad (5)$$

Where γ_m / m_m denotes the maximum value of grain boundary energy/grain boundary mobility at high angle grain boundaries other than those near the misorientation of the CSL boundary; θ, the misorientation; θ_0, the misorientation of the CSL boundary where the grain boundary energy and grain boundary mobility are minimum; θ_m, the range of angles in which neither the grain boundary energy nor the grain boundary mobility is maximum; and n and B are parameters. We assumed $n = 4$ and $B = 5$. Equation (4) shows the Read–Shockley relationship. θ_m is determined by Brandon deviation angle $\theta_m(\Sigma) = (\pi/12)/\sqrt{\Sigma}$, where Σ denotes the order of CSL boundary.[12)]

3. Time Evolution of Artificial Texture

3.1 Simulation data and simulation conditions

Under three different grain boundary conditions, the proposed grain growth model was applied to simulate the grain growth of an artificial texture wherein initial randomly oriented grains were all square in form. Under Condition (A), the grain boundary energy and grain boundary mobility were assumed to remain the same regardless of the misorientation. Under Conditions (B) and (C), consideration was given to the $\Sigma 1$ boundary and high-angle grain boundaries close to 60 degrees. The minimum value for high-angle grain boundary energy and mobility, respectively, was assumed to be 30% of the maximum value, and the angle range was assumed to be 15 degrees under Condition (B) and 25 degrees under Condition (C).

Fig. 2 shows the grain boundary energy and grain boundary mobility relative to the misorientation. Microstructures used in the simulation are also shown in Fig. 2. The simulated region is 210 μm × 216 μm, in which 5,040 squares approximately 3 μm × 3 μm in size are arranged. The form of initial grains was assumed to be square because it facilitates preparing simulation data. Because quadruple junctions need to be divided into two triple junctions, the quadrangles were intentionally assumed to be non-square. The division of quadruple junctions into triple junctions can be done by following the rule inferred from the topological transformation of triple junctions.[10)] The Euler angle for each grain was given at random. As shown in Fig. 2, the misorientation distribution in the initial state is a Mackenzie distribution, indicating that the Euler angle was properly given to the grains at random.[13)]

3.2 Simulation results and consideration

3.2.1 Time evolution of average grain area

As a result of our simulation using the proposed model, we could confirm that the average grain area, or the square of average grain diameter, is proportional to time, as shown in Fig. 2. Thus, the same simulation results as obtainable in the absence of any inhibitor that pins the grain boundaries, or with a curvature model applied to continuous grain growth, could be obtained. From Equation (1) that expresses the migration of grain boundaries, it is considered that the factor of proportionality, or the rate of grain growth, can be correlated to the product of grain boundary mobility and grain boundary energy. From the simulation results, the ratio of time evolution of the average grain area among the simulation conditions was (A):(B):(C) = 1.00:0.72:0.54. On the other hand, the ratio of the square of the average product of grain boundary mobility and grain boundary energy, weighted by misorientation distribution, was (A):(B):(C) = 1.00:0.85:0.67. Although the rate of grain growth in the simulation can roughly be predicted from the grain boundary property, it may be said that the actual rate of grain growth is higher than the prediction. This is considered due to the results described in 3.2.2.

3.2.2 Change of misorientation distribution

When the grain boundary property are constant (Condition (A)), the misorientation distribution remains almost the same. On the other hand, when the grain boundary property vary according to the misorientation (Conditions (B) and (C)), the misorientation distribution differs markedly from that under Condition (A) (Fig. 2). In the region where the grain boundary mobility and grain boundary energy decrease, the frequency of misorientation, or grain boundary length increases. Elsewhere, the frequency of misorientation decreases. Although there is little difference in the amount of change in frequency of misorientation between Conditions (B) and (C), under Condition (C) where the angle range in which the grain boundary property vary widens, the amount of change in frequency of misorientation in the neighborhood of $\Sigma 1$ that shows small misorientation is a little larger than that under Condition (B). Therefore, it may be said that the angle range, too, influences the change in frequency of misorientation. The change in frequency of misorientation is considered to influence the rate of grain growth as well.

4. Comparison between Results of Experiment Using Actual Material and Results of Simulation

4.1 Experimental conditions and simulation conditions

First, a steel ingot containing 0.5%Si and 0.5%Mn was prepared

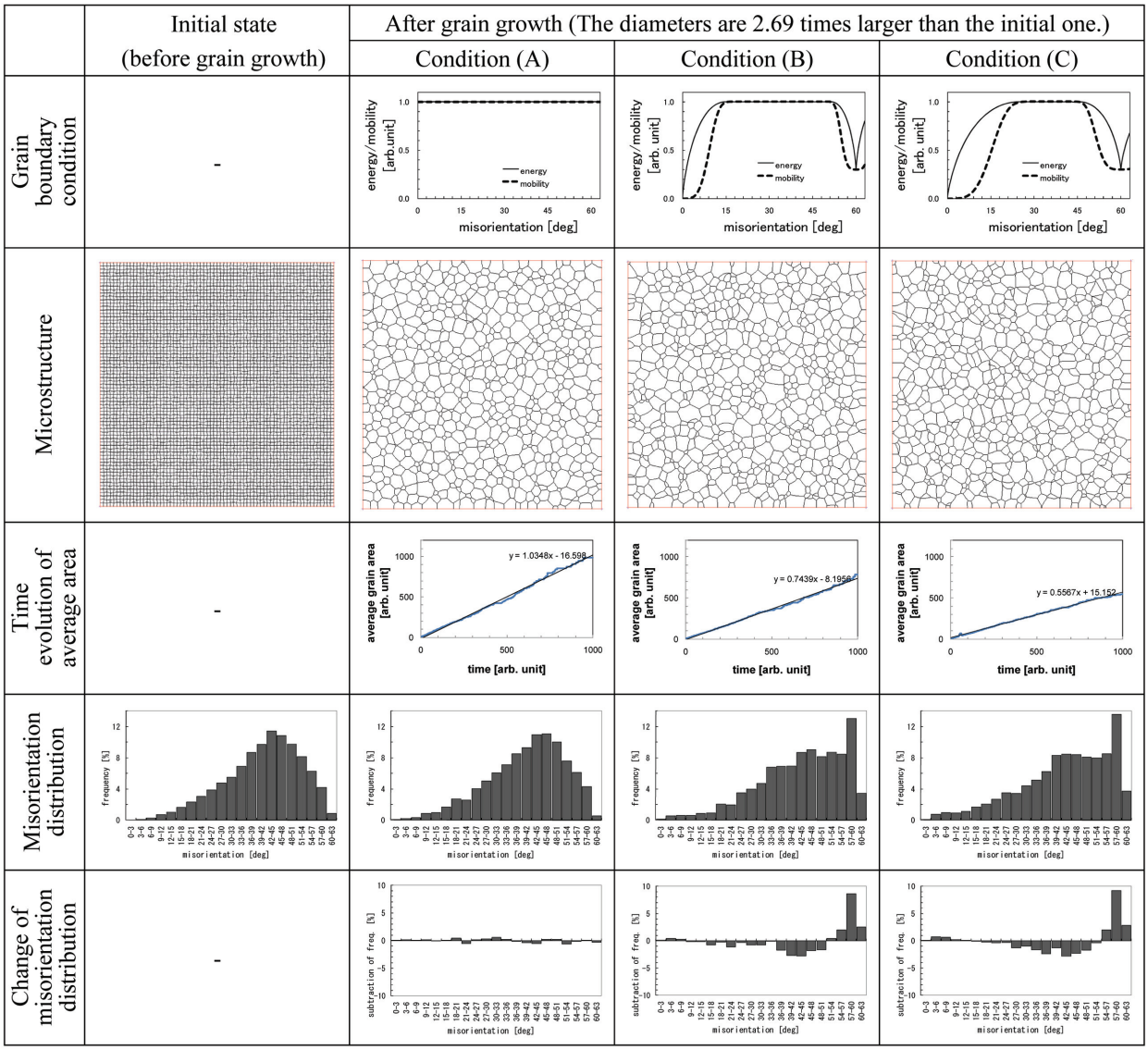

Fig. 2 Conditions and results of grain growth simulation on each grain boundary
Condition (A): Constant boundary characteristics. Condition (B): Σ1 boundary and high angle grain boundaries close to 60˚ are taken into account. The angle range is 15˚. Condition (C): Σ1 boundary and high angle grain boundaries close to 60˚ are taken into account. The angle range is 25˚.

using a vacuum melting process. After the ingot was annealed at 1,150˚C for one hour, it was hot-rolled into a 2.3-mm-thick sheet. Next, the sheet was cold rolled to a thickness of 0.5 mm. Then, the cold-rolled sheet was annealed at 730˚C for 30 seconds to complete the recrystallization. That specimen was assumed to be in the initial state. The specimen was further subjected to 30-second annealing at 730˚C, 780˚C and 830˚C, respectively, to consider three different states after the grain growth.

An EBSD observation was made at the ND plane at the sheet thickness center. The textures measured were: (1) general texture (1,000 points 12-mm wide, 10-mm long specimen measured manually to collect data) and (2) local texture (orientation mapping width 600 μm × length 1,800 μm, in 3-μm step, for grain growth simulation). As the initial microstructure for the grain growth simulation, the orientation mapping data (point elements) of (2) above from the specimen in initial state transformed into linear elements was used. Concerning the equations of grain boundary energy and grain boundary mobility, consideration was given only to the Σ1 grain boundary ($\theta_0 = 0^\circ$, $\theta_m = 15^\circ$) and high-angle grain boundary ($\theta_0 = 60^\circ$, $\theta_m = 8.7^\circ$) (Condition (B)) on the basis of Reference 11.

4.2 Results and consideration

Figs. 3-5 show the experimental results obtained after grain growth by 30-second annealing at 780˚C and equivalent simulation results. Concerning the misorientation distribution after grain growth, the simulation results agree relatively well with the experimental results (Fig. 3). With respect to the grain size distribution, the results agree fairly well except for small grains (Fig. 4). Looking at the change in texture, the experimental results show a marked intensification of the {111}//ND orientation with the grain growth, whereas the simulation results do not show much change in texture, though

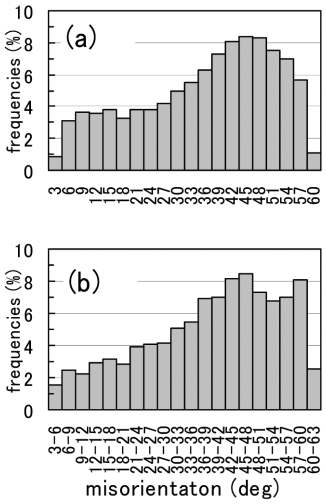

Fig. 3 Misorientation distributions after grain growth
(a) Experiment (b) Simulation

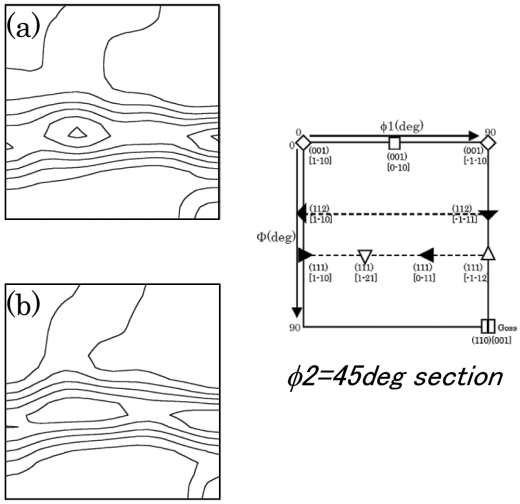

Fig. 5 Textures after grain growth
(a) Experiment (b) Simulation

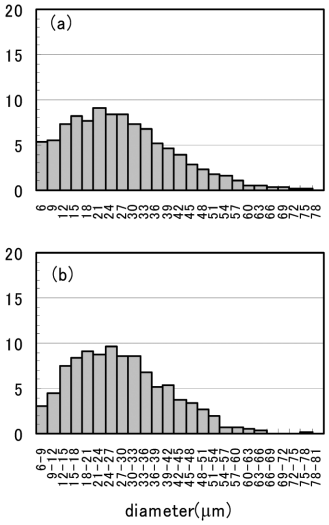

Fig. 4 Grain size distributions after grain growth
(a) Experiment (b) Simulation

they show a similar tendency (Fig. 5).

From the above results, it can be said that our model simulates the experimental results relatively well. The differences that are found between the experimental results and simulation results are considered due to the fact that the grain growth model used for the simulation was a two-dimensional one and that the grain boundary property used in the simulation were different from those used in the experiment.

5. Conclusion

We developed a new local curvature multi-vertex model to simulate the grain growth. It is a two-dimensional topological network model that directly expresses the physical principles concerning the curvature of grain boundaries and the grain boundary tension at triple junctions.

Through an analysis of the time evolution of an artificial texture and a comparison between experimental results and simulation results, we determined the validity and applicability of the developed model. Specifically, it was confirmed that the grain growth follows the law of time to the half power derived from a classical curvature model, that the grain boundary property influences the change in misorientation distribution and the rate of grain growth, and that the developed model can simulate the experimental results relatively well. The differences found between the experimental and simulation results are considered due to the fact that the developed grain growth model is two-dimensional and that the grain boundary property assumed in the simulation were different from those used in the experiment.

In the future, we intend to make a detailed study of continuous and discontinuous grain growth using the developed simulation model and thereby contribute to further sophistication of the steel materials Nippon Steel Corporation offers.

References

1) Ushigami, Y., Nakayama, T.: Mater. Sci. Forum. 157, 1081 (1994)
2) Wright, S. I., Nowell, M. M.: Microsc. Microanal. 12, 72 (2006)
3) Anderson, M. P., Srolovitz, D. J., Grest, G. S., Sahni, P. S.: Acta Metall. 32, 783 (1984)
4) Fan, D., Chen, L. Q.: Acta Mater. 45, 611 (1997)
5) Frost, H. J., Thompson, C. V., Howe, C. L., Whang, J.: Scripta Metall. 22, 65 (1988)
6) Frost, H. J., Thompson, C. V., Walton, D. T.: Acta Metall. Mater. 38 (8), 1455 (1990)
7) Soares, A., Ferro, A. C., Fortes, M. A.: Scripta Metall. 19, 1491 (1985)
8) Kawasaki, K., Nagai, T., Nagashima, K.: Phil. Mag. B. 60 (3), 399 (1989)
9) Fuchizaki, K., Kusaba, T., Kawasaki, K.: Phil. Mag. B. 71 (3), 333 (1995)
10) Weygand, D., Bréchet, Y., Léepinoux, J.: Phil. Mag. B. 78 (4), 392 (1998)
11) Humphreys, F. J.: Acta mater. 45 (10), 4231 (1997)
12) Brandon, D. G.: Acta Metall. 14, 1479 (1966)
13) Mackenzie, J. K.: Biometrika. 45, 229 (1958)

Teruyuki TAMAKI
Chief Researcher
Hirohata R&D Lab.
1 Fuji-cho, Hirohata-ku, Himeji, Hyogo 671-1188

Kohsaku USHIODA
Fellow, Dr.Eng.
Technical Development Bureau

Kenichi MURAKAMI
Chief Researcher, Dr.
Hirohata R&D Lab.